Science Advances
AAAS

Supplementary Materials for

Ligands binding to the prion protein induce its proteolytic release with therapeutic potential in neurodegenerative proteinopathies

Luise Linsenmeier, Behnam Mohammadi, Mohsin Shafiq, Karl Frontzek, Julia Bär, Amulya N. Shrivastava, Markus Damme, Feizhi Song, Alexander Schwarz, Stefano Da Vela, Tania Massignan, Sebas-tian Jung, Angela Correia, Matthias Schmitz, Berta Puig, Simone Hornemann, Inga Zerr, Jörg Tatzelt, Emi-liano Biasini, Paul Saftig, Michaela Schweizer, Dmitri Svergun, Ladan Amin, Federica Mazzola, Luca Va-rani, Simrika Thapa, Sabine Gilch, Hermann Schätzl, David A. Harris, Antoine Triller, Marina Mikhaylova, Adriano Aguzzi, Hermann C. Altmeppen*, Markus Glatzel*

*Corresponding author. Email: h.altmeppen@uke.de (H.C.A.); m.glatzel@uke.de (M.G.)

Published 24 November 2021, *Sci. Adv.* **7**, eabj1826 (2021)
DOI: 10.1126/sciadv.abj1826

The PDF file includes:

Other Supplementary Material for this manuscript includes the following:

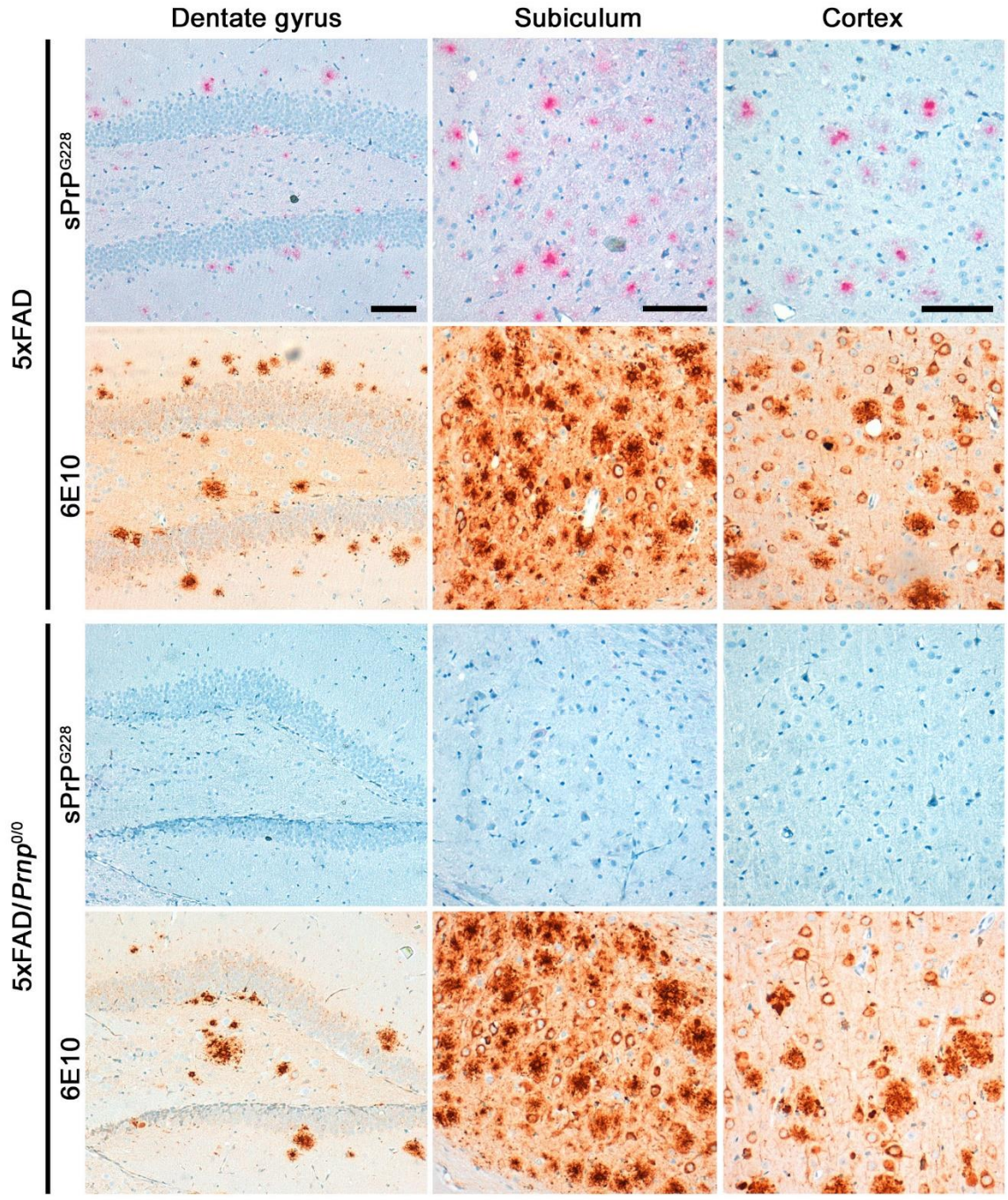

Fig. S1. Immunohistochemical assessment of sPrP and (human) Aβ/APP in different brain regions of 5xFAD and 5xFAD/*Prnp*$^{0/0}$ mice. Representative pictures showing areas of dentate gyrus, subiculum and cerebral cortex. Prominent Aβ plaques as well as cell-associated Aβ/APP are detected with the 6E10 antibody (DAB) in both genotypes, whereas (plaque-like) sPrP (using the sPrP^{G228} antibody) is only detected in 5xFAD mice with WT background (i.e., with PrP expression). This excludes unspecific binding of sPrP^{G228} (and/or the respective 2nd antibody used for detection) to Aβ deposits.

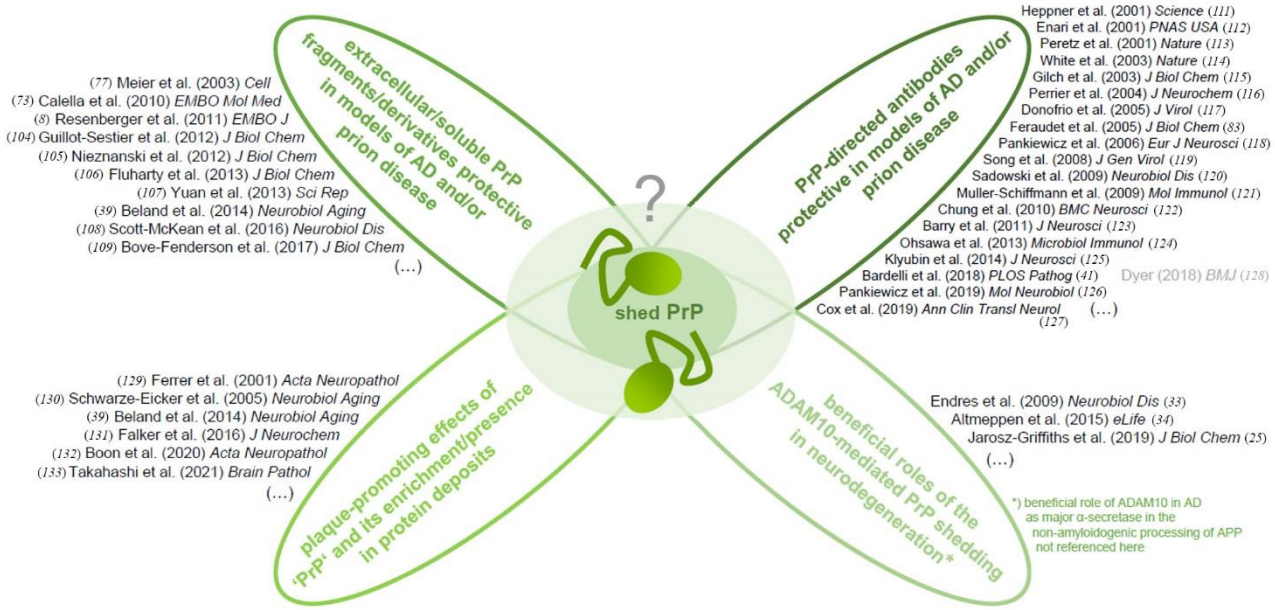

Fig. S2. Scheme combining different concepts of PrP-associated protection in neurodegenerative diseases and referencing important respective studies of various groups. While diverse mechanisms may be involved in these aspects, note that (I) protective roles of extracellular PrP forms/fragments (see references *8*, *39*, *73*, *77*, *101-110*), (II) beneficial effects of some PrP-directed antibodies (references *41*, *83*, *111-128*), (III) the plaque-promoting action of 'PrP' (references *39*, *129-133*), and (IV) protection by ADAM10 (references *25*, *33*, *34*) (besides its role as the major α-secretase in the non-amyloidogenic processing of APP not covered here) might all be connected by physiological PrP shedding and shed PrP (center). Further studies are clearly required to investigate this possible link.

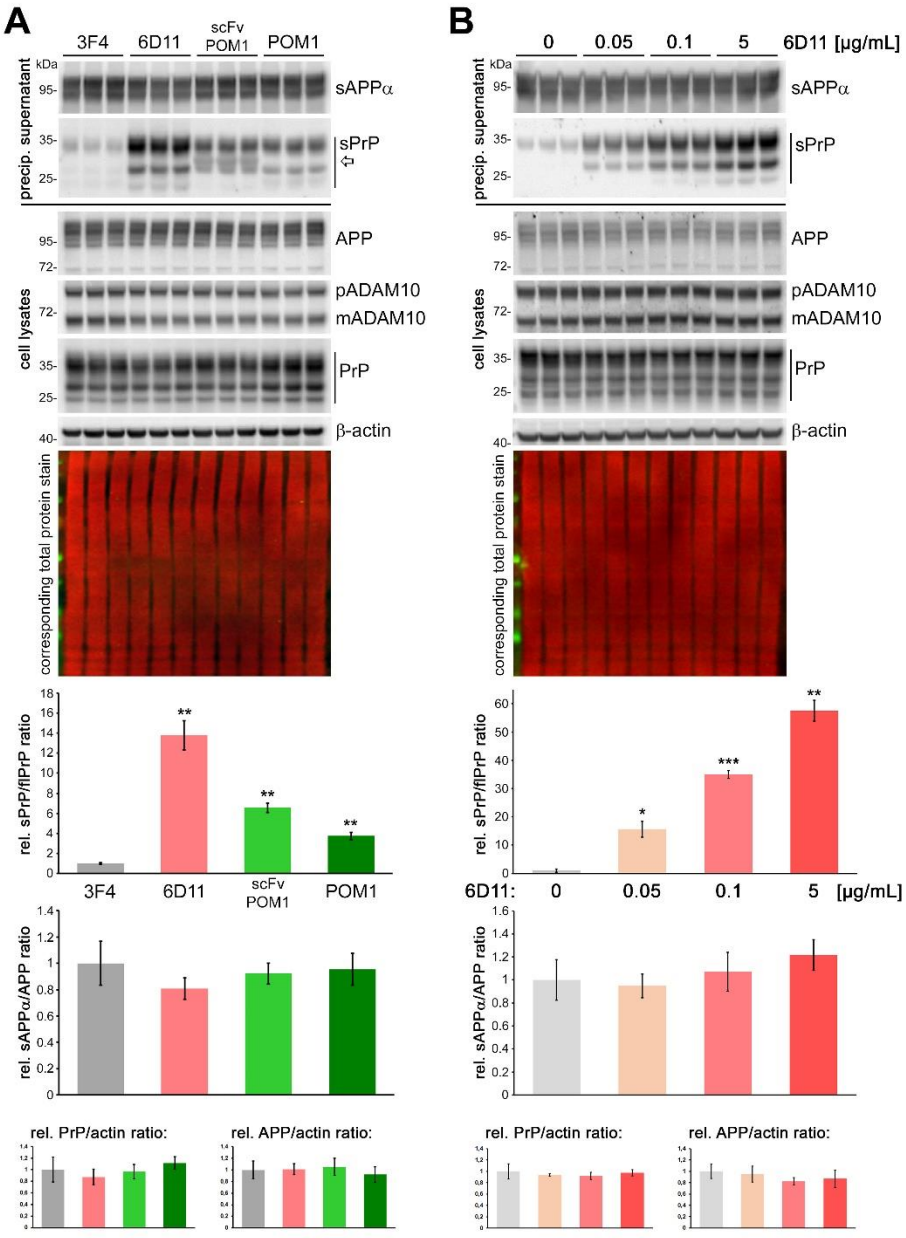

Fig. S3. A Biochemical assessment of sPrP and sAPPα (in precipitated conditioned media) and APP, ADAM10, and PrP (in corresponding cell lysates) upon overnight treatment of N2a cells (3 wells per condition) with 3F4 (negative control), 6D11, single-chain (scFv) and classical (IgG) POM1. Actin and total protein stain shown as loading controls. Quantifications of sPrP-to-PrP and sAPPα-to-APP ratios (as well as PrP-to-actin and APP-to-actin [small diagrams]) are shown below. All antibodies directed against mouse PrP significantly increased shedding compared to controls (3F4) without relevant effects on released sAPPα and cell-associated PrP and APP. (Arrow at the sPrP blot indicates presence of an unknown band in samples treated with scFvPOM1, which poses some degree of error to the quantification that should be considered). **B** Detection of aforementioned proteins upon overnight treatment of N2a cells (in triplicates) with ascending doses of 6D11 antibody. Quantifications presented below. Plotted data in **A** and **B** shows mean (controls set to 1) ± SE; Student's *t*-test results considered significant at $*p < 0.05$, $**p < 0.005$, $***p < 0.001$.

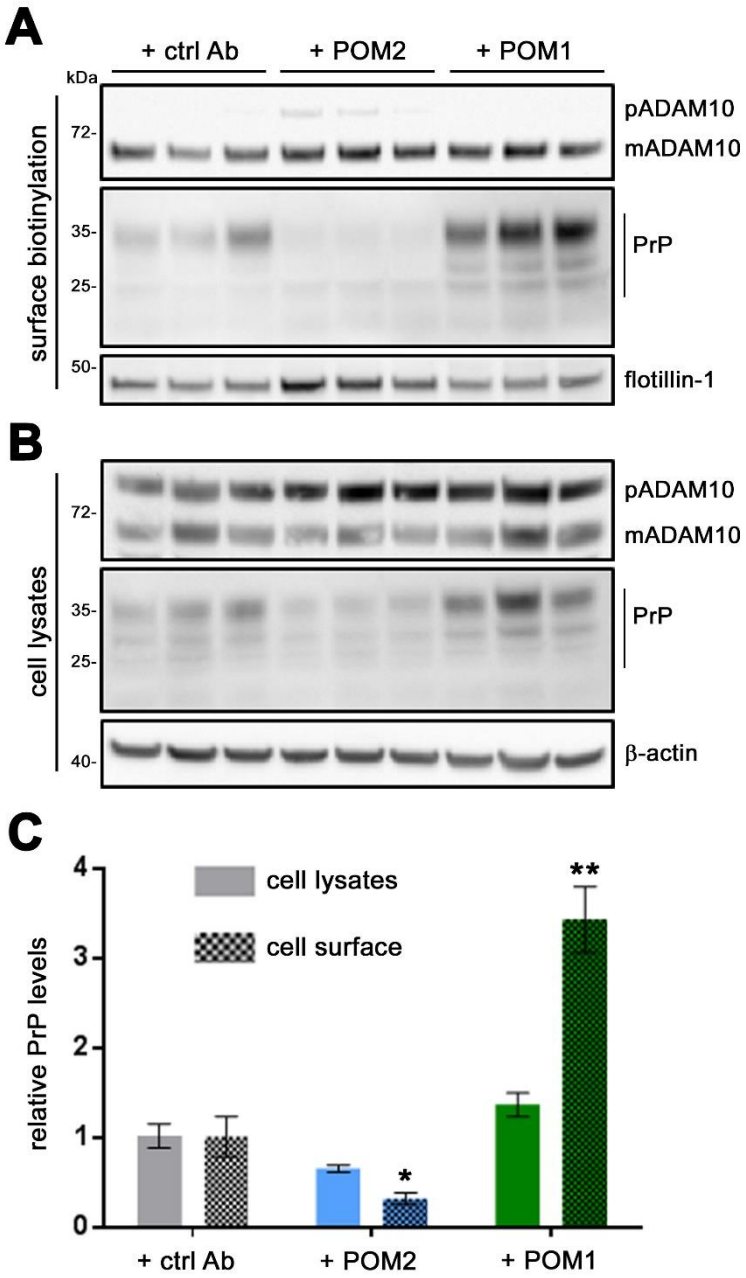

Fig. S4. Western blot analysis of a surface biotinylation assay (**A**) showing membrane levels of ADAM10 and PrP (flotillin shown as loading control) and corresponding total lysates (**B**) showing ADAM10 and PrP amounts (actin served as loading control) in N2a cells treated with POM2 or POM1 compared to cells treated with a non-PrP-directed control antibody. Quantification in **C** shows the relative levels of PrP in lysates (PrP/actin ratio) and at the cell surface (PrP/flotillin ratio; dotted graphs) with the respective control treatment set to 1. Note the decrease in PrP upon POM2 treatment, which is particularly pronounced at the cell surface. POM1 instead caused elevated PrP levels at the plasma membrane. Statistical analysis was carried out with n=3 for all experimental groups. For comparing cell surface PrP levels to the levels of PrP in lysates in each treatment, significance values were obtained by implementing one-way ANOVA followed by the Tukey post-hoc test. Plotted data shows mean ± SEM. *$p < 0.05$, **$p < 0.01$.

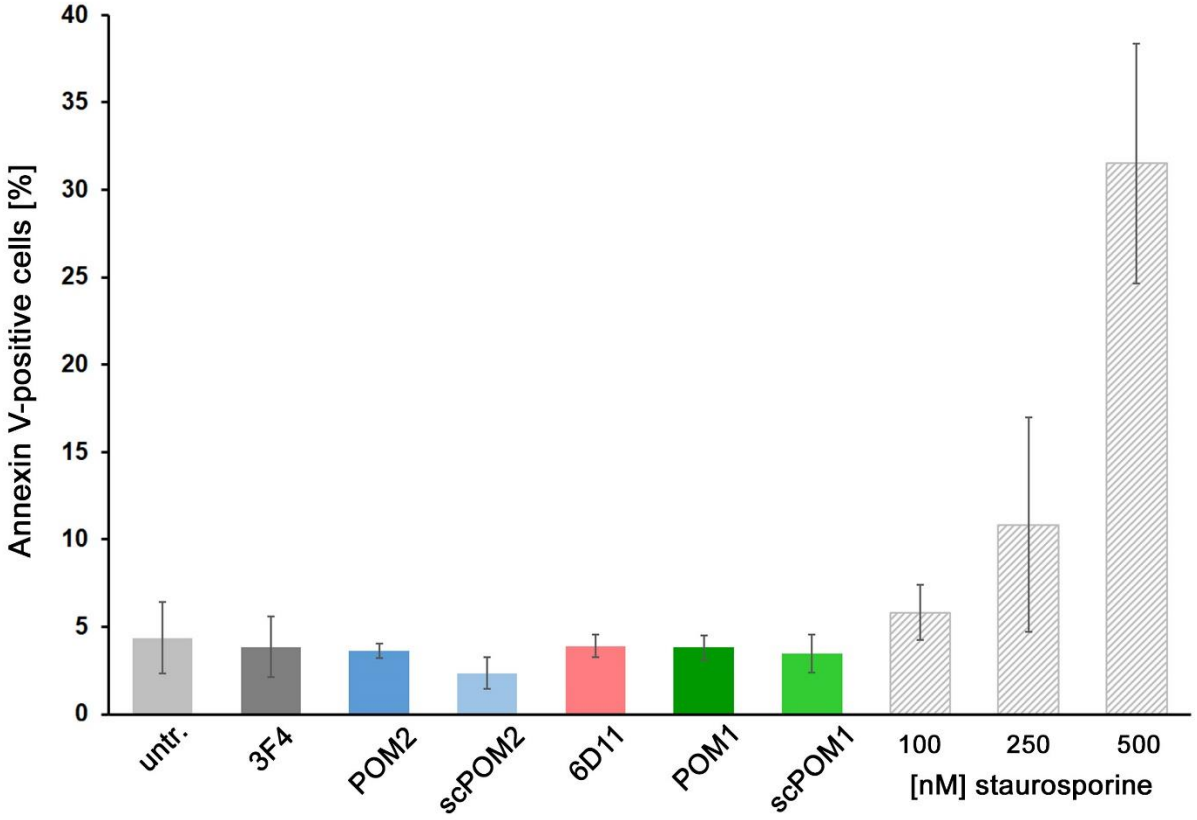

Fig. S5. Assessment of toxic effects of antibody treatments using an Annexin V apoptosis assay. Upon treatment with the indicated antibodies, the percentage of Annexin V-positive cells was determined by FACS compared to untreated (untr.) or 3F4 IgG-treated negative controls (grey bars). Different concentrations of staurosporine were used as positive controls inducing cell death. Mean ± SE; n=3 independent experiments (except for for 250nM STS: n=2 due to an experimental outlier excluded from quantification).

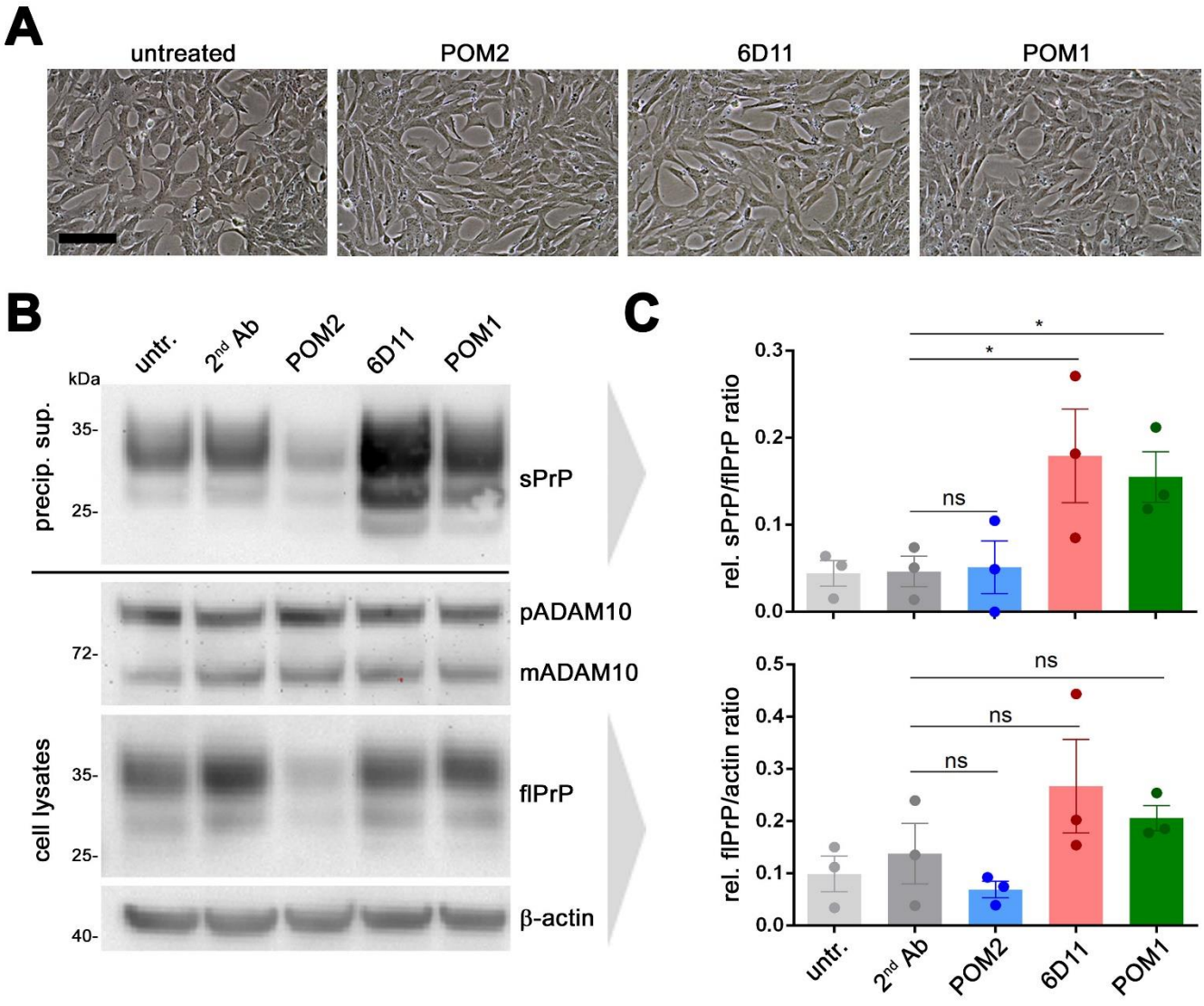

Fig. S6. Antibody-mediated effects on PrP shedding in the neuronal cell line mHippo E14. To confirm findings in N2a cells we performed the same treatments in another murine brain-derived cell line. **A** Incubation with antibodies did not alter overall cell density or morphology compared to untreated controls, thus suggesting lack of major toxicity (scale bar = 50 µm). **B** Representative western blot analysis showing similar changes caused by antibody treatment as observed in N2a cells (Figure 2C). However, while increased shedding was again observed upon 6D11 or POM1 treatment, the reduction of total PrP caused by POM2, albeit detectable, was not significant after quantification of n=3 independent experiments (graphs represent mean ± SEM) shown in **C**. Graphpad Prism (6.01) was used for calculating statistical significance in multiple comparisons by one-way ANOVA and uncorrected Fisher's LSD test (*$p < 0.05$).

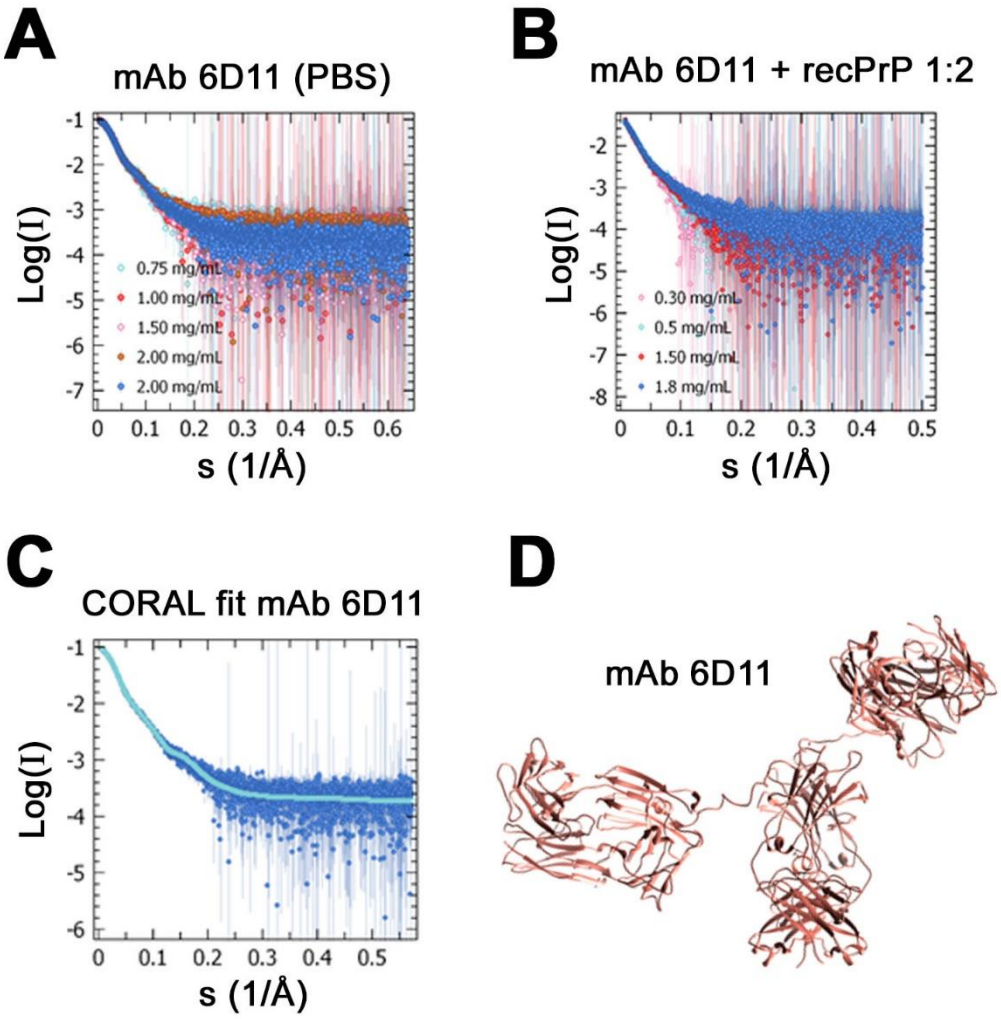

Fig. S7. SAXS profiles for the concentration series of (**A**) 6D11 antibody and (**B**) recPrP (23–230) / 6D11 antibody complex (in a 2:1 ratio). **C**, **D** SAXS data and modelling of the 6D11 antibody. **C** Experimental SAXS profile (symbols) and CORAL fit (solid line) for the representative model of the 6D11 antibody (χ^2=0.85). **D** A typical model of the 6D11 antibody obtained with CORAL from the IgG2a crystal structure 1igt.pdb allowing for a flexible hinge region (the model was further used for the modelling of the recPrP/6D11 complex shown in Fig. 4). For further detail also refer to Table S1 and its associated information.

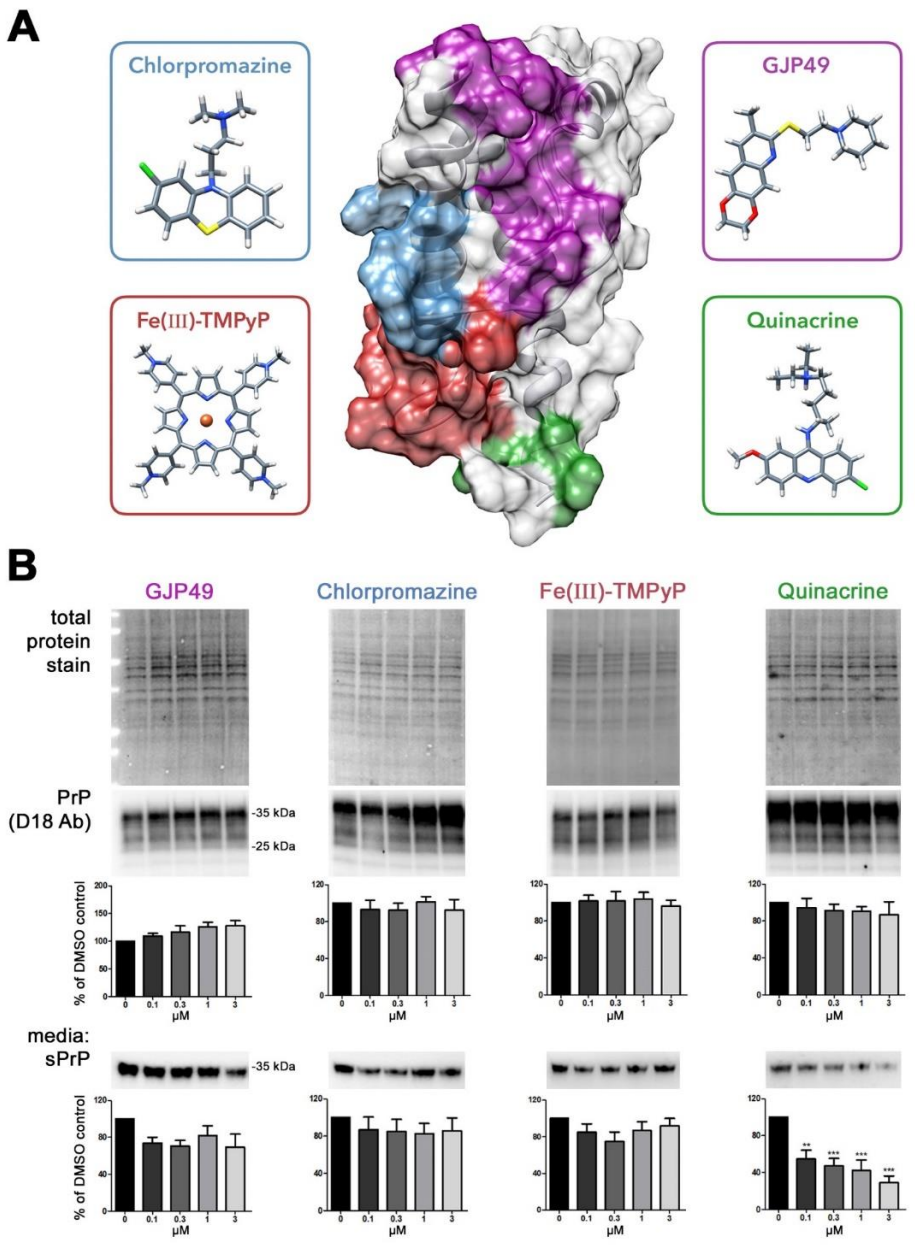

Fig. S8. No shedding-stimulating activity of four PrP-directed chemical compounds. **A** Structural representation of four known PrP-binding compounds (framed boxes) and their expected binding regions (coloured regions) within the globular part of PrP (center). **B** Biochemical assessment of total proteins (as loading control) and PrP levels in lysates as well as sPrP in corresponding media supernatants of HEK293 cells stably expressing murine PrP and treated with increasing concentrations of the respective substance (indicated). Densitometric quantifications of at least four independent experiments are shown under the representative blots. PrP signals (detected with D18 or $sPrP^{G228}$ antibody) were normalized to the signal of total proteins in cell lysates. Bar graphs show PrP or sPrP levels expressed as the mean percentage of untreated (DMSO only) controls ± standard errors. Data was processed with the Prism software, version 7.0 (GraphPad) and analyzed with one-way ANOVA test, Dunnett`s post-hoc test; *p*-values are indicated as **<0.01, ***<0.001.

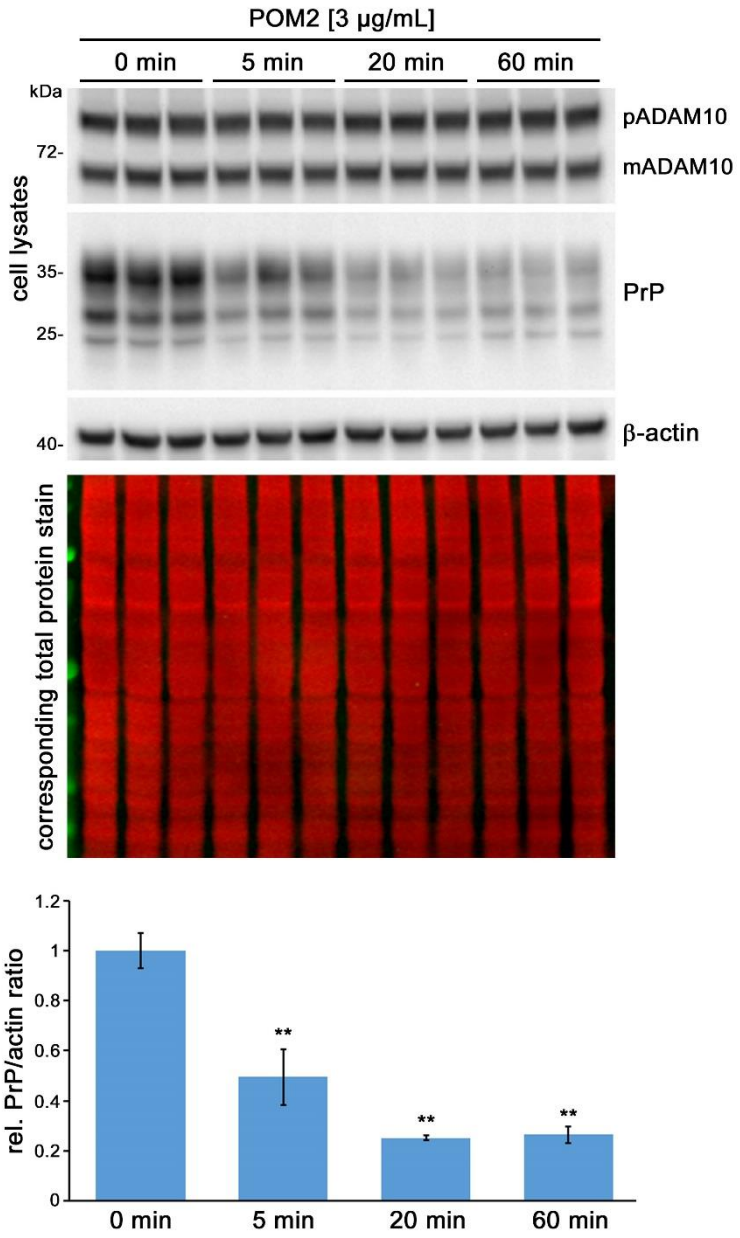

Fig. S9. POM2 treatment time course. Western blot analysis showing PrP, ADAM10 and β-actin in N2a cells treated for the indicated duration with POM2 antibody (3 wells per condition). Total protein stain shown as additional loading control. Quantifications of PrP-to-actin ratios shown below. POM2 caused a relatively quick reduction cellular PrP levels which then stabilized at low levels after 20 min. Plotted data shows mean (controls at 0 min set to 1) ± SE; Student's *t*-test results considered significant at $*p < 0.05$, $**p < 0.005$; significances calculated compared to the 0 min time-point.

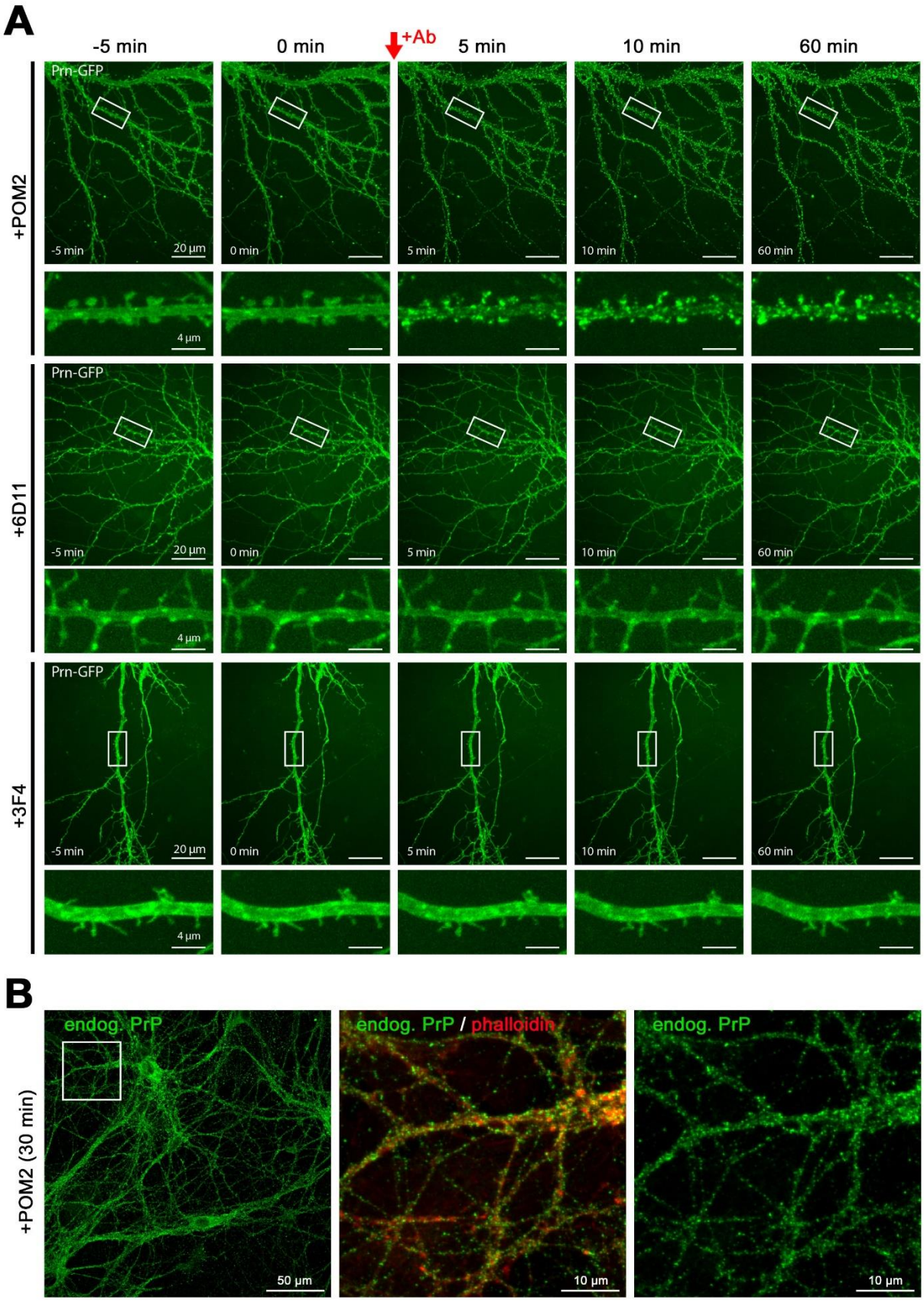
A
-5 min
0 min
+Ab
5 min
10 min
60 min
+POM2
+6D11
+3F4
Prn-GFP
20 µm
4 µm
B
+POM2 (30 min)
endog. PrP
endog. PrP / phalloidin
50 µm
10 µm

Fig. S10. Fluorescence microscopy demonstrating POM2-mediated clustering of PrP. **A** Live-microscopy pictures (see also Movie S1) of rat hippocampal neurons expressing GFP-tagged PrP (green) taken shortly before (left two columns; -5 and 0 min) and after (right three columns; 5, 10 and 60 min) treatment with POM2, 6D11 or 3F4 antibody (start of treatment indicated by red arrow). Overviews showing neuronal dendritic trees (scale bars = 20 µm) are followed by magnified view on individual dendrites indicated by white frames (scale bar in close-ups is 4 µm). Note that a strong clustering of PrP (green) is only detectable upon treatment with POM2. **B** IF analysis of WT rat neurons fixed after 30 min of POM2 treatment and stained for PrP (green) reveals that POM2-mediated clustering also occurs on endogenous PrP. Phalloidin (red) was used to stain actin for better display of neuronal processes.

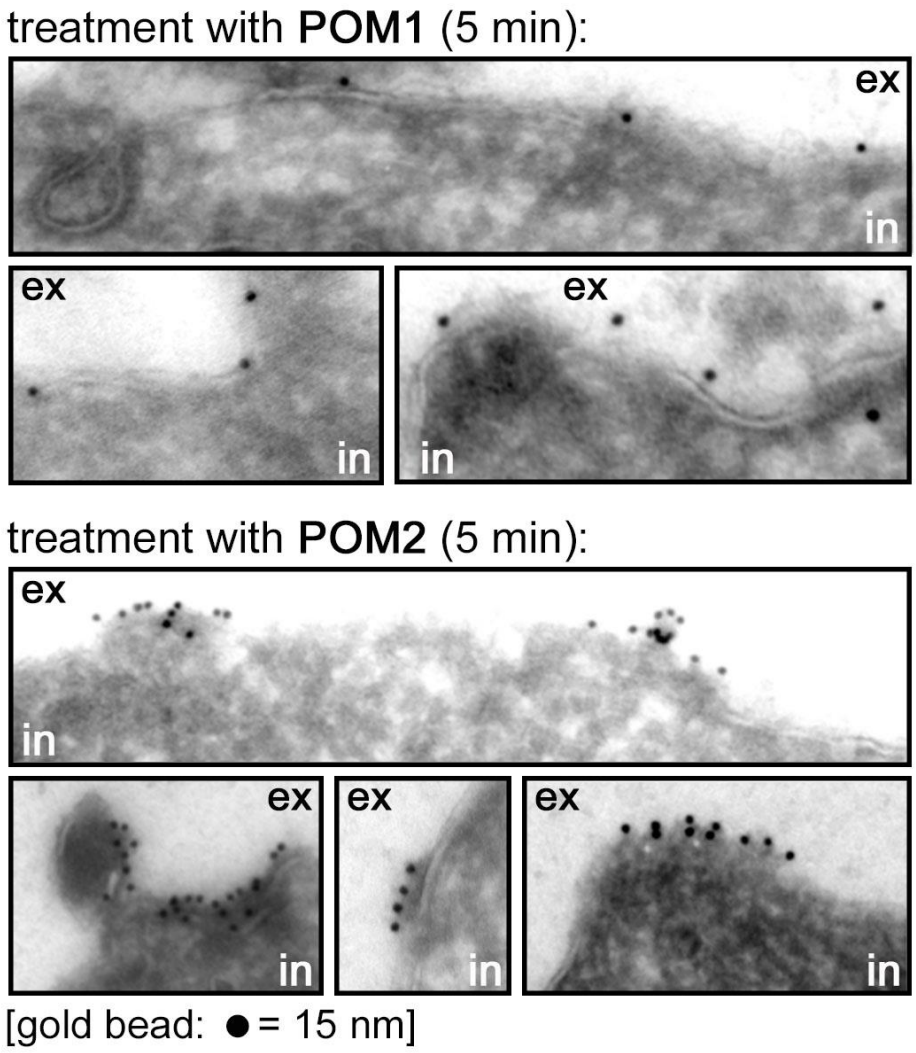

Fig. S11. Immuno-EM comparison between N2a cells treated for 5 min with either POM1 or POM2. Immunogold-positive clusters were exclusively observed in samples incubated with POM2 (lower panel), whereas treatment with equal amounts of POM1 only resulted in isolated dots (upper panel). In this set of experiments, pan-PrP antibody 6D11 was used for detection, followed by a rabbit anti-mouse secondary antibody and protein A coupled to 10 nm colloidal gold. Ex: extracellular; in: intracellular.

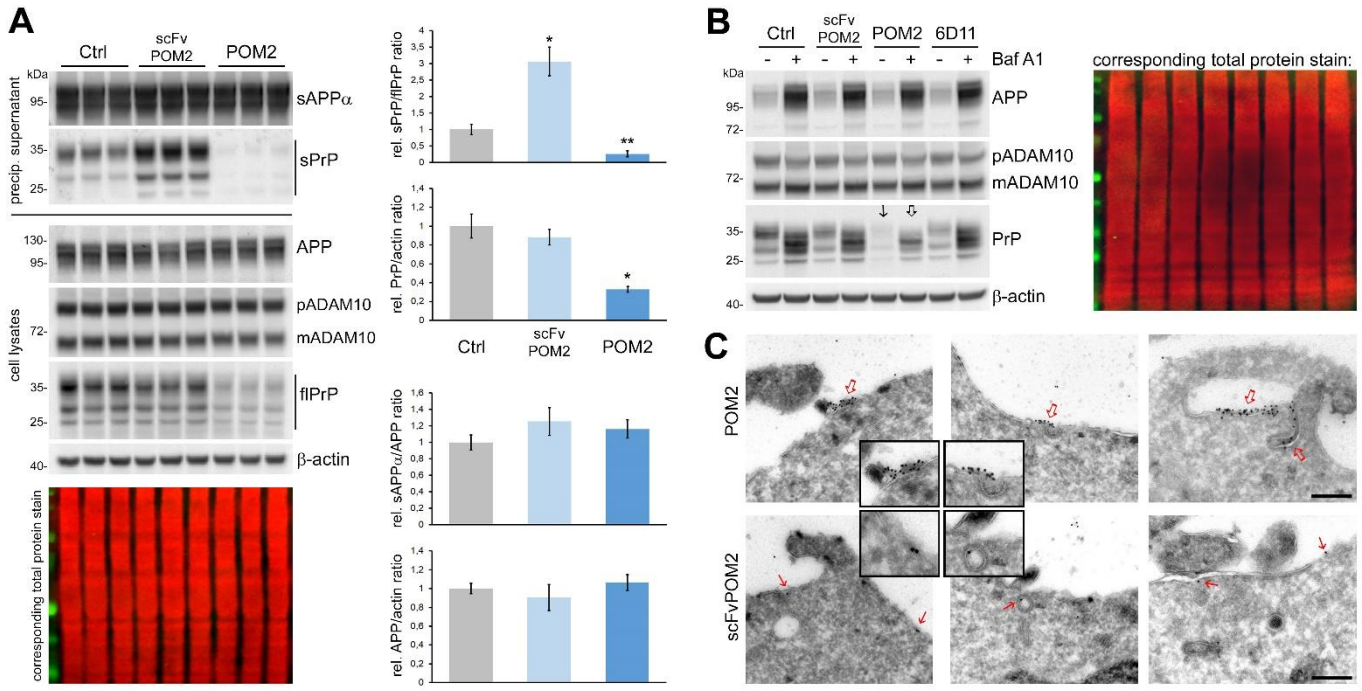

Fig. S12. Comparison of effects of single-chain POM2 and POM2 IgG in N2a cells. **A** Western blot analysis of sPrP and sAPPα (in precipitated conditioned media) and APP, ADAM10, and PrP (in corresponding cell lysates) upon overnight treatment (3 wells per condition) with scFvPOM2 or POM2 IgG. Actin and total protein stain serving as loading controls. Quantifications of sPrP-to-PrP, sAPPα-to-APP, PrP-to-actin and APP-to-actin ratios are shown on the right. Single-chain POM2 caused increased shedding, whereas POM2 caused significant reductions in sPrP and cellular PrP levels compared to untreated controls (sAPPα and APP levels remained largely unaltered). Plotted data shows mean (controls set to 1) ± SE; Student's *t*-test results considered significant at $*p < 0.05$, $**p < 0.005$. **B** Co-treatment with PrP-directed antibodies and Bafilomycin (for lysosomal inhibition). Treatment with Baf A1 (+) consistently causes an increase in both, PrP and APP levels, compared to non-Baf A1 treatment (-). However, while cells incubated with single-chain POM2 (scFvPOM2) share a similar pattern with cells treated with no antibody (Ctrl) or with 6D11, Baf A1 in POM2-treated cells causes reappearance (bold arrow) of the otherwise largely vanished PrP signal (thin arrow), consistent with data in Fig. 6B. Actin and total protein stain serving as loading controls. **C** Immuno-EM comparison between cells treated for 10 min with POM2 or scFvPOM2. Immunogold-positive clusters were exclusively and consistently observed for POM2 treatment (upper panel; bold red arrows and magnifications highlight representative clusters at the surface and instances of invagination/uptake), whereas corresponding amounts of scFvPOM2 only resulted in sparse individual signals (lower panel) at the cell surface and occasionally in intracellular compartments (red thin arrows and magnified detail). Detection was with 6D11 followed by protein A-coupled gold; scale bars represent 200 nm.

Table S1. SAXS data collection, parameters and additional information.

Data collection parameters			
Radiation source	Petra III (DESY)		
Beamline	EMBL P12		
Detector	Pilatus 6M		
Wavelength (nm)	0.124		
Sample-detector distance (m)	3		
s range (nm^{-1})	0.03 - 7.3		
Exposure time (s)	6 (=60 x 0.1 s) or 2 (=20 x 0.1 s)		
Temperature (K)	293.2		
Overall parameters	**recPrP**	**6D11**	**Complex 2:1**
Concentration (mg/mL)	1.56	2.00	1.80
R_g from Guinier approximation (nm)	2.78 ± 0.04	5.12 ± 0.03	8.13 ± 0.02
R_g from PDDF* (nm)	2.9 ± 0.1	5.23 ± 0.09	7.60 ± 0.02
Max.Intramolecular distance D_{MAX} (nm)	9.9	17.6	24.8
Porod Volume, V_P (nm^3)	43	330	954
Molecular weight, I(0) (kDa)	n/a	120	206
Molecular weight from Bayesian estimate (kDa)	20.8 - 24	127 - 151	221 - 373
Expected molecular weight (e.g. sequence) (kDa)	22.9	150**	196
Software employed			
Primary data reduction	SASFLOW		
Data processing	PRIMUS		
Hybrid (rigid/random loops) and Rigid body modelling	CORAL, SASpy		

*Pair distance distribution function
**Typical IgG molecular mass

Supplementary information on SAXS measurements and data

SAXS data and modelling for pure **recPrP** accounting for its partial disorder are reported in detail elsewhere (SASBDB accession code: SASDHV9). The overall SAXS-derived parameters of recPrP are presented in Table S1, and an ensemble of CORAL models and their best fit to the data are shown in Fig. 4A,C (25% of conformers shown for clarity). The significant variability of the N-terminal parts in these models suggests that recPrP, distal to the membrane anchoring site, samples multiple conformations including very extended ones. The **6D11** antibody is a murine IgG2a. The SAXS profiles of the concentration series displayed in fig. S7 overlap well, thus pointing to the absence of interparticle interactions in the concentration range probed here. In the following, the curve at 2 mg/mL, with the best signal to noise ratio, was employed. The derived overall parameters (Table S1) are indicative of a typical monomeric IgG. In order to model the conformation of 6D11, the crystal structure of another murine IgG2a (*134*), PDB accession code 1IGT, was employed. The conformation in the crystal structure does not fit satisfactorily the SAXS data (discrepancy χ^2=2.84, not shown). To obtain representative conformations for the solution state, the model was disconnected in the constituting Fab and Fc domains, and the hinge region of the heavy chains modelled in CORAL as two 20 amino acids long random loops. Ten independent CORAL reconstructions consistently revealed an approximately T-shaped conformation fitting the data well (χ^2=0.84-0.87) (fig. S7), and thus yielding a representative model of the dominant antibody conformer in solution.

The concentration series of the 2:1 recPrP/6D11-antibody complex also shows consistently overlapping curves without concentration-dependent effects (fig. S7B). The complex was modelled against the representative data set collected at 1.8 mg/mL. The overall parameters (Table S1) suggest a rather extended assembly and a representative model of a 2:1 complex, with χ^2=0.83, modelled on the basis of these data is shown in Fig. 4D. Intriguingly, to explain the SAXS data, the complex had to be modelled by using very extended conformers for recPrP. While complex formation with such a flexible antigen will almost certainly result in multiple conformations, the solution scattering pattern is dominated by “open” conformations of the complex. This suggests that, in the presence of the 6D11 antibody, PrP (as assessed here for recPrP) tends to adopt predominantly extended conformations.

Table S2. SPT-QD analysis.

Median Diffusion Coefficient, D ($\mu m^2/s$) for data plotted in **Fig. 7B** and **7D**.

Three experiments performed on independent cultures. Total number of QDs analyzed per condition.

Kolmogorov-Smirnov test comparing the distribution of diffusion coefficient values.

		POM1 (control)	POM1 (1 h)	POM19 (control)	POM19 (1 h)	POM2 (control)	POM2 (1 h)	POM11 (control)	POM11 (1 h)	POM3 (control)	POM3 (1h)
SYNAPTIC	**Median D**	0.1010	0.0858	0.1008	0.0912	0.1067	0.0555	0.0961	0.0518	0.0956	0.0740
	No. of QDs	428	591	383	302	213	115	350	288	155	102
	KS-test	**		ns		***		***		ns	
EXTRA-SYNAPTIC											
	Median D	0.1594	0.1404	0.1790	0.1505	0.1865	0.1015	0.1560	0.0980	0.1385	0.1421
	No. of QDs	2439	2985	1757	1950	915	571	1192	1187	770	577
	KS-test	***		***		***		***		***	

Movie S1. Time-resolved compilation of a representative live microscopy analysis of PrP-GFP-expressing rat neurons treated with POM2 (left), 6D11 (center) or 3F4 (right) antibodies (parts of it are highlighted in Fig. 6 and fig. S10A). Note the strong clustering of PrP upon POM2 administration visible all over the selected dendritic tree.

REFERENCES AND NOTES

1. A. Aguzzi, C. Haass, Games played by rogue proteins in prion disorders and Alzheimer's disease. *Science* **302**, 814–818 (2003).

2. J. Vaquer-Alicea, M. I. Diamond, Propagation of protein aggregation in neurodegenerative diseases. *Annu. Rev. Biochem.* **88**, 785–810 (2019).

3. F. Checler, B. Vincent, Alzheimer's and prion diseases: Distinct pathologies, common proteolytic denominators. *Trends Neurosci.* **25**, 616–620 (2002).

4. I. Benilova, B. De Strooper, Prion protein in Alzheimer's pathogenesis: A hot and controversial issue. *EMBO Mol. Med.* **2**, 289–290 (2010).

5. J. Lauren, D. A. Gimbel, H. B. Nygaard, J. W. Gilbert, S. M. Strittmatter, Cellular prion protein mediates impairment of synaptic plasticity by amyloid-β oligomers. *Nature* **457**, 1128–1132 (2009).

6. S. B. Prusiner, Novel proteinaceous infectious particles cause scrapie. *Science* **216**, 136–144 (1982).

7. C. Weissmann, Molecular biology of prion diseases. *Trends Cell Biol.* **4**, 10–14 (1994).

8. U. K. Resenberger, A. Harmeier, A. C. Woerner, J. L. Goodman, V. Müller, R. Krishnan, R. M. Vabulas, H. A. Kretzschmar, S. Lindquist, F. U. Hartl, G. Multhaup, K. F. Winklhofer, J. Tatzelt, The cellular prion protein mediates neurotoxic signalling of β-sheet-rich conformers independent of prion replication. *EMBO J.* **30**, 2057–2070 (2011).

9. D. G. Ferreira, M. Temido-Ferreira, H. V. Miranda, V. L. Batalha, J. E. Coelho, É. M. Szegö, I. Marques-Morgado, S. H. Vaz, J. S. Rhee, M. Schmitz, I. Zerr, L. V. Lopes, T. F. Outeiro, α-synuclein interacts with PrP^{C} to induce cognitive impairment through mGluR5 and NMDAR2B. *Nat. Neurosci.* **20**, 1569–1579 (2017).

10. T. Ondrejcak, I. Klyubin, G. T. Corbett, G. Fraser, W. Hong, A. J. Mably, M. Gardener, J. Hammersley, M. S. Perkinton, A. Billinton, D. M. Walsh, M. J. Rowan, Cellular prion protein

mediates the disruption of hippocampal synaptic plasticity by soluble tau in vivo. *J. Neurosci.* **38**, 10595–10606 (2018).

11. G. T. Corbett, Z. Wang, W. Hong, M. Colom-Cadena, J. Rose, M. Liao, A. Asfaw, T. C. Hall, L. Ding, A. DeSousa, M. P. Frosch, J. Collinge, D. A. Harris, M. S. Perkinton, T. L. Spires-Jones, T. L. Young-Pearse, A. Billinton, D. M. Walsh, PrP is a central player in toxicity mediated by soluble aggregates of neurodegeneration-causing proteins. *Acta Neuropathol.* **139**, 503–526 (2020).

12. L. M. Smith, M. A. Kostylev, S. Lee, S. M. Strittmatter, Systematic and standardized comparison of reported amyloid-β receptors for sufficiency, affinity, and Alzheimer's disease relevance. *J. Biol. Chem.* **294**, 6042–6053 (2019).

13. M. Beland, X. Roucou, The prion protein unstructured N-terminal region is a broad-spectrum molecular sensor with diverse and contrasting potential functions. *J. Neurochem.* **120**, 853–868 (2012).

14. C. R. Trevitt, L. L. P. Hosszu, M. Batchelor, S. Panico, C. Terry, A. J. Nicoll, E. Risse, W. A. Taylor, M. K. Sandberg, H. al-Doujaily, J. M. Linehan, H. R. Saibil, D. J. Scott, J. Collinge, J. P. Waltho, A. R. Clarke, N-terminal domain of prion protein directs its oligomeric association. *J. Biol. Chem.* **289**, 25497–25508 (2014).

15. N. S. Rösener, L. Gremer, M. M. Wördehoff, T. Kupreichyk, M. Etzkorn, P. Neudecker, W. Hoyer, Clustering of human prion protein and α-synuclein oligomers requires the prion protein N-terminus. *Commun. Biol.* **3**, 365 (2020).

16. J. W. Um, A. C. Kaufman, M. Kostylev, J. K. Heiss, M. Stagi, H. Takahashi, M. E. Kerrisk, A. Vortmeyer, T. Wisniewski, A. J. Koleske, E. C. Gunther, H. B. Nygaard, S. M. Strittmatter, Metabotropic glutamate receptor 5 is a coreceptor for Alzheimer Aβ oligomer bound to cellular prion protein. *Neuron* **79**, 887–902 (2013).

17. R. Linden, The biological function of the prion protein: A cell surface scaffold of signaling modules. *Front. Mol. Neurosci.* **10**, 77 (2017).

18. H. Büeler, A. Raeber, A. Sailer, M. Fischer, A. Aguzzi, C. Weissmann, High prion and PrPSc levels but delayed onset of disease in scrapie-inoculated mice heterozygous for a disrupted PrP gene. *Mol. Med.* **1**, 19–30 (1994).

19. M. K. Sandberg, H. Al-Doujaily, B. Sharps, A. R. Clarke, J. Collinge, Prion propagation and toxicity in vivo occur in two distinct mechanistic phases. *Nature* **470**, 540–542 (2011).

20. A. Sailer, H. Büeler, M. Fischer, A. Aguzzi, C. Weissmann, No propagation of prions in mice devoid of PrP. *Cell* **77**, 967–968 (1994).

21. G. Mallucci, A. Dickinson, J. Linehan, P. C. Klöhn, S. Brandner, J. Collinge, Depleting neuronal PrP in prion infection prevents disease and reverses spongiosis. *Science* **302**, 871–874 (2003).

22. M. D. White, M. Farmer, I. Mirabile, S. Brandner, J. Collinge, G. R. Mallucci, Single treatment with RNAi against prion protein rescues early neuronal dysfunction and prolongs survival in mice with prion disease. *Proc. Natl. Acad. Sci. U.S.A.* **105**, 10238–10243 (2008).

23. N. C. Ferreira, L. M. Ascari, A. G. Hughson, G. R. Cavalheiro, C. F. Góes, P. N. Fernandes, J. R. Hollister, R. A. da Conceição, D. S. Silva, A. M. T. Souza, M. L. C. Barbosa, F. A. Lara, R. A. P. Martins, B. Caughey, Y. Cordeiro, A promising antiprion trimethoxychalcone binds to the globular domain of the cellular prion protein and changes its cellular location. *Antimicrob. Agents Chemother.* **62**, e01441-17 (2018).

24. G. J. Raymond, H. T. Zhao, B. Race, L. D. Raymond, K. Williams, E. E. Swayze, S. Graffam, J. le, T. Caron, J. Stathopoulos, R. O'Keefe, L. L. Lubke, A. G. Reidenbach, A. Kraus, S. L. Schreiber, C. Mazur, D. E. Cabin, J. B. Carroll, E. V. Minikel, H. Kordasiewicz, B. Caughey, S. M. Vallabh, Antisense oligonucleotides extend survival of prion-infected mice. *JCI Insight* **5**, e131175 (2019).

25. H. H. Jarosz-Griffiths, N. J. Corbett, H. A. Rowland, K. Fisher, A. C. Jones, J. Baron, G. J. Howell, S. A. Cowley, S. Chintawar, M. Z. Cader, K. A. B. Kellett, N. M. Hooper, Proteolytic shedding of the prion protein via activation of metallopeptidase ADAM10 reduces cellular binding and toxicity of amyloid-β oligomers. *J. Biol. Chem.* **294**, 7085–7097 (2019).

26. L. Linsenmeier, B. Mohammadi, S. Wetzel, B. Puig, W. S. Jackson, A. Hartmann, K. Uchiyama, S. Sakaguchi, K. Endres, J. Tatzelt, P. Saftig, M. Glatzel, H. C. Altmeppen, Structural and mechanistic aspects influencing the ADAM10-mediated shedding of the prion protein. *Mol. Neurodegener.* **13**, 18 (2018).

27. D. R. Borchelt, M. Rogers, N. Stahl, G. Telling, S. B. Prusiner, Release of the cellular prion protein from cultured cells after loss of its glycoinositol phospholipid anchor. *Glycobiology* **3**, 319–329 (1993).

28. D. R. Taylor, E. T. Parkin, S. L. Cocklin, J. R. Ault, A. E. Ashcroft, A. J. Turner, N. M. Hooper, Role of ADAMs in the ectodomain shedding and conformational conversion of the prion protein. *J. Biol. Chem.* **284**, 22590–22600 (2009).

29. H. C. Altmeppen, J. Prox, B. Puig, M. A. Kluth, C. Bernreuther, D. Thurm, E. Jorissen, B. Petrowitz, U. Bartsch, B. de Strooper, P. Saftig, M. Glatzel, Lack of a-disintegrin-and-metalloproteinase ADAM10 leads to intracellular accumulation and loss of shedding of the cellular prion protein in vivo. *Mol. Neurodegener.* **6**, 36 (2011).

30. S. Lammich, E. Kojro, R. Postina, S. Gilbert, R. Pfeiffer, M. Jasionowski, C. Haass, F. Fahrenholz, Constitutive and regulated alpha-secretase cleavage of Alzheimer's amyloid precursor protein by a disintegrin metalloprotease. *Proc. Natl. Acad. Sci. U.S.A.* **96**, 3922–3927 (1999).

31. D. Hartmann, B. de Strooper, L. Serneels, K. Craessaerts, A. Herreman, W. Annaert, L. Umans, T. Lübke, A. Lena Illert, K. von Figura, P. Saftig, The disintegrin/metalloprotease ADAM 10 is essential for Notch signalling but not for alpha-secretase activity in fibroblasts. *Hum. Mol. Genet.* **11**, 2615–2624 (2002).

32. K. Endres, F. Fahrenholz, J. Lotz, C. Hiemke, S. Teipel, K. Lieb, O. Tuscher, A. Fellgiebel, Increased CSF APPs-α levels in patients with Alzheimer disease treated with acitretin. *Neurology* **83**, 1930–1935 (2014).

33. K. Endres, G. Mitteregger, E. Kojro, H. Kretzschmar, F. Fahrenholz, Influence of ADAM10 on prion protein processing and scrapie infectiosity in vivo. *Neurobiol. Dis.* **36**, 233–241 (2009).

34. H. C. Altmeppen, J. Prox, S. Krasemann, B. Puig, K. Kruszewski, F. Dohler, C. Bernreuther, A. Hoxha, L. Linsenmeier, B. Sikorska, P. P. Liberski, U. Bartsch, P. Saftig, M. Glatzel, The sheddase ADAM10 is a potent modulator of prion disease. *eLife* **4**, e04260 (2015).

35. P. Saftig, S. F. Lichtenthaler, The alpha secretase ADAM10: A metalloprotease with multiple functions in the brain. *Prog. Neurobiol.* **135**, 1–20 (2015).

36. M. Shi, K. Dennis, J. J. Peschon, R. Chandrasekaran, K. Mikecz, Antibody-induced shedding of CD44 from adherent cells is linked to the assembly of the cytoskeleton. *J. Immunol.* **167**, 123–131 (2001).

37. F. Schelter, J. Kobuch, M. L. Moss, J. D. Becherer, P. M. Comoglio, C. Boccaccio, A. Krüger, A disintegrin and metalloproteinase-10 (ADAM-10) mediates DN30 antibody-induced shedding of the met surface receptor. *J. Biol. Chem.* **285**, 26335–26340 (2010).

38. M. Hartmann, L. M. Parra, A. Ruschel, C. Lindner, H. Morrison, A. Herrlich, P. Herrlich, Inside-out regulation of ectodomain cleavage of cluster-of-differentiation-44 (CD44) and of neuregulin-1 requires substrate dimerization. *J. Biol. Chem.* **290**, 17041–17054 (2015).

39. M. Beland, M. Bedard, G. Tremblay, P. Lavigne, X. Roucou, Aβ induces its own prion protein N-terminal fragment (PrPN1)-mediated neutralization in amorphous aggregates. *Neurobiol. Aging* **35**, 1537–1548 (2014).

40. M. Polymenidou, R. Moos, M. Scott, C. Sigurdson, Y. Z. Shi, B. Yajima, I. Hafner-Bratkovič, R. Jerala, S. Hornemann, K. Wuthrich, A. Bellon, M. Vey, G. Garen, M. N. G. James, N. Kav, A. Aguzzi, The POM monoclonals: A comprehensive set of antibodies to non-overlapping prion protein epitopes. *PLOS ONE* **3**, e3872 (2008).

41. M. Bardelli, K. Frontzek, L. Simonelli, S. Hornemann, M. Pedotti, F. Mazzola, M. Carta, V. Eckhardt, R. D'Antuono, T. Virgilio, S. F. González, A. Aguzzi, L. Varani, A bispecific immunotweezer prevents soluble PrP oligomers and abolishes prion toxicity. *PLOS Pathog.* **14**, e1007335 (2018).

42. J. Falsig, T. Sonati, U. S. Herrmann, D. Saban, B. Li, K. Arroyo, B. Ballmer, P. P. Liberski, A. Aguzzi, Prion pathogenesis is faithfully reproduced in cerebellar organotypic slice cultures. *PLOS Pathog.* **8**, e1002985 (2012).

43. M. Beland, J. Motard, A. Barbarin, X. Roucou, PrP(C) homodimerization stimulates the production of PrPC cleaved fragments PrPN1 and PrPC1. *J. Neurosci.* **32**, 13255–13263 (2012).

44. A. D. Engelke, A. Gonsberg, S. Thapa, S. Jung, S. Ulbrich, R. Seidel, S. Basu, G. Multhaup, M. Baier, M. Engelhard, H. M. Schätzl, K. F. Winklhofer, J. Tatzelt, Dimerization of the cellular prion protein inhibits propagation of scrapie prions. *J. Biol. Chem.* **293**, 8020–8031 (2018).

45. L. Carter, S. J. Kim, D. Schneidman-Duhovny, J. Stöhr, G. Poncet-Montange, T. M. Weiss, H. Tsuruta, S. B. Prusiner, A. Sali, Prion protein-antibody complexes characterized by chromatography-coupled small-angle x-ray scattering. *Biophys. J.* **109**, 793–805 (2015).

46. T. Sonati, R. R. Reimann, J. Falsig, P. K. Baral, T. O'Connor, S. Hornemann, S. Yaganoglu, B. Li, U. S. Herrmann, B. Wieland, M. Swayampakula, M. H. Rahman, D. Das, N. Kav, R. Riek, P. P. Liberski, M. N. G. James, A. Aguzzi, The toxicity of antiprion antibodies is mediated by the flexible tail of the prion protein. *Nature* **501**, 102–106 (2013).

47. A. P. Le Brun, C. L. Haigh, S. C. Drew, M. James, M. P. Boland, S. J. Collins, Neutron reflectometry studies define prion protein N-terminal peptide membrane binding. *Biophys. J.* **107**, 2313–2324 (2014).

48. U. S. Herrmann, T. Sonati, J. Falsig, R. R. Reimann, P. Dametto, T. O'Connor, B. Li, A. Lau, S. Hornemann, S. Sorce, U. Wagner, D. Sanoudou, A. Aguzzi, Prion infections and anti-PrP antibodies trigger converging neurotoxic pathways. *PLOS Pathog.* **11**, e1004662 (2015).

49. B. Wu, A. J. McDonald, K. Markham, C. B. Rich, K. P. McHugh, J. Tatzelt, D. W. Colby, G. L. Millhauser, D. A. Harris, The N-terminus of the prion protein is a toxic effector regulated by the C-terminus. *eLife* **6**, e23473 (2017).

50. S. L. Shyng, M. T. Huber, D. A. Harris, A prion protein cycles between the cell surface and an endocytic compartment in cultured neuroblastoma cells. *J. Biol. Chem.* **268**, 15922–15928 (1993).

51. M. L. Barreca, N. Iraci, S. Biggi, V. Cecchetti, E. Biasini, Pharmacological agents targeting the cellular prion protein. *Pathogens* **7**, 27 (2018).

52. Y. O. Kamatari, Y. Hayano, K. Yamaguchi, J. Hosokawa-Muto, K. Kuwata, Characterizing antiprion compounds based on their binding properties to prion proteins: Implications as medical chaperones. *Protein Sci.* **22**, 22–34 (2013).

53. P. K. Baral, M. Swayampakula, M. K. Rout, N. N. V. Kav, L. Spyracopoulos, A. Aguzzi, M. N. G. James, Structural basis of prion inhibition by phenothiazine compounds. *Structure* **22**, 291–303 (2014).

54. C. Stincardini, T. Massignan, S. Biggi, S. R. Elezgarai, V. Sangiovanni, I. Vanni, M. Pancher, V. Adami, J. Moreno, M. Stravalaci, G. Maietta, M. Gobbi, A. Negro, J. R. Requena, J. Castilla, R. Nonno, E. Biasini, An antipsychotic drug exerts anti-prion effects by altering the localization of the cellular prion protein. *PLOS ONE* **12**, e0182589 (2017).

55. S. A. Priola, A. Raines, W. S. Caughey, Porphyrin and phthalocyanine antiscrapie compounds *Science* **287**, 1503–1506 (2000).

56. T. Massignan, S. Cimini, C. Stincardini, M. Cerovic, I. Vanni, S. R. Elezgarai, J. Moreno, M. Stravalaci, A. Negro, V. Sangiovanni, E. Restelli, G. Riccardi, M. Gobbi, J. Castilla, T. Borsello, R. Nonno, E. Biasini, A cationic tetrapyrrole inhibits toxic activities of the cellular prion protein. *Sci. Rep.* **6**, 23180 (2016).

57. C. Korth, B. C. H. May, F. E. Cohen, S. B. Prusiner, Acridine and phenothiazine derivatives as pharmacotherapeutics for prion disease. *Proc. Natl. Acad. Sci. U.S.A.* **98**, 9836–9841 (2001).

58. M. Vogtherr, S. Grimme, B. Elshorst, D. M. Jacobs, K. Fiebig, C. Griesinger, R. Zahn, Antimalarial drug quinacrine binds to C-terminal helix of cellular prion protein. *J. Med. Chem.* **46**, 3563–3564 (2003).

59. S. Biggi, M. Pancher, C. Stincardini, S. Luotti, T. Massignan, A. Dalle Vedove, A. Astolfi, P. Gatto, G. Lolli, M. L. Barreca, V. Bonetto, V. Adami, E. Biasini, Identification of compounds inhibiting

prion replication and toxicity by removing PrP^C from the cell surface. *J. Neurochem.* **152**, 136–150 (2020).

60. S. M. Vallabh, C. K. Nobuhara, F. Llorens, I. Zerr, P. Parchi, S. Capellari, E. Kuhn, J. Klickstein, J. G. Safar, F. C. Nery, K. J. Swoboda, M. D. Geschwind, H. Zetterberg, S. E. Arnold, E. V. Minikel, S. L. Schreiber, Prion protein quantification in human cerebrospinal fluid as a tool for prion disease drug development. *Proc. Natl. Acad. Sci. U.S.A.* **116**, 7793–7798 (2019).

61. E. V. Minikel, H. T. Zhao, J. le, J. O'Moore, R. Pitstick, S. Graffam, G. A. Carlson, M. P. Kavanaugh, J. Kriz, J. B. Kim, J. Ma, H. Wille, J. Aiken, D. McKenzie, K. Doh-ura, M. Beck, R. O'Keefe, J. Stathopoulos, T. Caron, S. L. Schreiber, J. B. Carroll, H. B. Kordasiewicz, D. E. Cabin, S. M. Vallabh, Prion protein lowering is a disease-modifying therapy across prion disease stages, strains and endpoints. *Nucleic Acids Res.* **48**, 10615–10631 (2020).

62. A. Triller, D. Choquet, New concepts in synaptic biology derived from single-molecule imaging. *Neuron* **59**, 359–374 (2008).

63. P. Aguilar-Calvo, A. M. Sevillano, J. Bapat, K. Soldau, D. R. Sandoval, H. C. Altmeppen, L. Linsenmeier, D. P. Pizzo, M. D. Geschwind, H. Sanchez, B. S. Appleby, M. L. Cohen, J. G. Safar, S. D. Edland, M. Glatzel, K. P. R. Nilsson, J. D. Esko, C. J. Sigurdson, Shortening heparan sulfate chains prolongs survival and reduces parenchymal plaques in prion disease caused by mobile, ADAM10-cleaved prions. *Acta Neuropathol.* **139**, 527–546 (2020).

64. J. Kanaani, S. B. Prusiner, J. Diacovo, S. Baekkeskov, G. Legname, Recombinant prion protein induces rapid polarization and development of synapses in embryonic rat hippocampal neurons in vitro. *J. Neurochem.* **95**, 1373–1386 (2005).

65. L. Amin, X. T. Nguyen, I. G. Rolle, E. D'Este, G. Giachin, T. H. Tran, V. Č. Šerbec, D. Cojoc, G. Legname, Characterization of prion protein function by focal neurite stimulation. *J. Cell Sci.* **129**, 3878–3891 (2016).

66. B. W. Megra, E. A. Eugenin, J. W. Berman, The role of shed PrP^c in the neuropathogenesis of HIV infection. *J. Immunol.* **199**, 224–232 (2017).

67. S. Martellucci, C. Santacroce, F. Santilli, L. Piccoli, S. Delle Monache, A. Angelucci, R. Misasi, M. Sorice, V. Mattei, Cellular and molecular mechanisms mediated by recPrP^{C} involved in the neuronal differentiation process of mesenchymal stem cells. *Int. J. Mol. Sci.* **20**, 345 (2019).

68. E. Mantuano, P. Azmoon, M. A. Banki, M. S. Lam, C. J. Sigurdson, S. L. Gonias, A soluble derivative of PrP^{C} activates cell-signaling and regulates cell physiology through LRP1 and the NMDA receptor. *J. Biol. Chem.* **295**, 14178–14188 (2020).

69. A. Küffer, A. K. K. Lakkaraju, A. Mogha, S. C. Petersen, K. Airich, C. Doucerain, R. Marpakwar, P. Bakirci, A. Senatore, A. Monnard, C. Schiavi, M. Nuvolone, B. Grosshans, S. Hornemann, F. Bassilana, K. R. Monk, A. Aguzzi, The prion protein is an agonistic ligand of the G protein-coupled receptor Adgrg6. *Nature* **536**, 464–468 (2016).

70. L. T. Haas, S. V. Salazar, M. A. Kostylev, J. W. Um, A. C. Kaufman, S. M. Strittmatter, Metabotropic glutamate receptor 5 couples cellular prion protein to intracellular signalling in Alzheimer's disease. *Brain* **139**, 526–546 (2016).

71. H. H. Jarosz-Griffiths, E. Noble, J. V. Rushworth, N. M. Hooper, Amyloid-β receptors: The good, the bad and the prion protein. *J. Biol. Chem.* **291**, 3174–3183 (2016).

72. N. W. Hu, A. J. Nicoll, D. Zhang, A. J. Mably, T. O'Malley, S. A. Purro, C. Terry, J. Collinge, D. M. Walsh, M. J. Rowan, mGlu5 receptors and cellular prion protein mediate amyloid-β-facilitated synaptic long-term depression in vivo. *Nat. Commun.* **5**, 3374 (2014).

73. A. M. Calella, M. Farinelli, M. Nuvolone, O. Mirante, R. Moos, J. Falsig, I. M. Mansuy, A. Aguzzi, Prion protein and Aβ-related synaptic toxicity impairment. *EMBO Mol. Med.* **2**, 306–314 (2010).

74. A. R. Foley, G. P. Roseman, K. Chan, A. Smart, T. S. Finn, K. Yang, R. S. Lokey, G. L. Millhauser, J. A. Raskatov, Evidence for aggregation-independent, PrP^{C}-mediated Aβ cellular internalization. *Proc. Natl. Acad. Sci. U.S.A.* **117**, 28625–28631 (2020).

75. L. Solforosi, J. R. Criado, D. B. McGavern, S. Wirz, M. Sánchez-Alavez, S. Sugama, L. A. DeGiorgio, B. T. Volpe, E. Wiseman, G. Abalos, E. Masliah, D. Gilden, M. B. Oldstone, B. Conti,

R. A. Williamson, Cross-linking cellular prion protein triggers neuronal apoptosis in vivo. *Science* **303**, 1514–1516 (2004).

76. L. M. Parra, M. Hartmann, S. Schubach, Y. Li, P. Herrlich, A. Herrlich, Distinct intracellular domain substrate modifications selectively regulate ectodomain cleavage of NRG1 or CD44. *Mol. Cell. Biol.* **35**, 3381–3395 (2015).

77. P. Meier, N. Genoud, M. Prinz, M. Maissen, T. Rülicke, A. Zurbriggen, A. J. Raeber, A. Aguzzi, Soluble dimeric prion protein binds PrP(Sc) in vivo and antagonizes prion disease. *Cell* **113**, 49–60 (2003).

78. B. Chesebro, M. Trifilo, R. Race, K. Meade-White, C. Teng, R. LaCasse, L. Raymond, C. Favara, G. Baron, S. Priola, B. Caughey, E. Masliah, M. Oldstone, Anchorless prion protein results in infectious amyloid disease without clinical scrapie. *Science* **308**, 1435–1439 (2005).

79. M. L. DeMarco, V. Daggett, Characterization of cell-surface prion protein relative to its recombinant analogue: Insights from molecular dynamics simulations of diglycosylated, membrane-bound human prion protein. *J. Neurochem.* **109**, 60–73 (2009).

80. C. J. Cheng, H. Koldso, M. W. Van der Kamp, B. Schiott, V. Daggett, Simulations of membrane-bound diglycosylated human prion protein reveal potential protective mechanisms against misfolding. *J. Neurochem.* **142**, 171–182 (2017).

81. M. V. Camacho, G. Telling, Q. Kong, P. Gambetti, S. Notari, Role of prion protein glycosylation in replication of human prions by protein misfolding cyclic amplification. *Lab. Invest.* **99**, 1741–1748 (2019).

82. H. E. Kang, J. Bian, S. J. Kane, S. Kim, V. Selwyn, J. Crowell, J. C. Bartz, G. C. Telling, Incomplete glycosylation during prion infection unmasks a prion protein epitope that facilitates prion detection and strain discrimination. *J. Biol. Chem.* **295**, 10420–10433 (2020).

83. C. Féraudet, N. Morel, S. Simon, H. Volland, Y. Frobert, C. Créminon, D. Vilette, S. Lehmann, J. Grassi, Screening of 145 anti-PrP monoclonal antibodies for their capacity to inhibit PrPSc replication in infected cells. *J. Biol. Chem.* **280**, 11247–11258 (2005).

84. A. G. Reidenbach, M. F. Mesleh, D. Casalena, S. M. Vallabh, J. L. Dahlin, A. J. Leed, A. I. Chan, D. L. Usanov, J. B. Yehl, C. T. Lemke, A. J. Campbell, R. N. Shah, O. K. Shrestha, J. R. Sacher, V. L. Rangel, J. A. Moroco, M. Sathappa, M. C. Nonato, K. T. Nguyen, S. K. Wright, D. R. Liu, F. F. Wagner, V. K. Kaushik, D. S. Auld, S. L. Schreiber, E. V. Minikel, Multimodal small-molecule screening for human prion protein binders. *J. Biol. Chem.* **295**, 13516–13531 (2020).

85. J. Falsig, A. Aguzzi, The prion organotypic slice culture assay—POSCA. *Nat. Protoc.* **3**, 555–562 (2008).

86. B. Mohammadi, L. Linsenmeier, M. Shafiq, B. Puig, G. Galliciotti, C. Giudici, M. Willem, T. Eden, F. Koch-Nolte, Y. H. Lin, J. Tatzelt, M. Glatzel, H. C. Altmeppen, Transgenic overexpression of the disordered prion protein N1 fragment in mice does not protect against neurodegenerative diseases due to impaired ER translocation. *Mol. Neurobiol.* **57**, 2812–2829 (2020).

87. B. van Bommel, A. Konietzny, O. Kobler, J. Bär, M. Mikhaylova, F-actin patches associated with glutamatergic synapses control positioning of dendritic lysosomes. *EMBO J.* **38**, e101183 (2019).

88. M. Renner, P. N. Lacor, P. T. Velasco, J. Xu, A. Contractor, W. L. Klein, A. Triller, Deleterious effects of amyloid β oligomers acting as an extracellular scaffold for mGluR5. *Neuron* **66**, 739–754 (2010).

89. A. N. Shrivastava, V. Redeker, L. Pieri, L. Bousset, M. Renner, K. Madiona, C. Mailhes-Hamon, A. Coens, L. Buée, P. Hantraye, A. Triller, R. Melki, Clustering of Tau fibrils impairs the synaptic composition of α3-Na^+/K^+-ATPase and AMPA receptors. *EMBO J.* **38**, e99871 (2019).

90. M. J. Saxton, K. Jacobson, Single-particle tracking: Applications to membrane dynamics. *Annu. Rev. Biophys. Biomol. Struct.* **26**, 373–399 (1997).

91. F. W. Studier, Protein production by auto-induction in high density shaking cultures. *Protein Expr. Purif.* **41**, 207–234 (2005).

92. C. E. Blanchet, A. Spilotros, F. Schwemmer, M. A. Graewert, A. Kikhney, C. M. Jeffries, D. Franke, D. Mark, R. Zengerle, F. Cipriani, S. Fiedler, M. Roessle, D. I. Svergun, Versatile sample

environments and automation for biological solution x-ray scattering experiments at the P12 beamline (PETRA III, DESY). *J. Appl. Cryst.* **48**, 431–443 (2015).

93. M. V. Petoukhov, D. Franke, A. V. Shkumatov, G. Tria, A. G. Kikhney, M. Gajda, C. Gorba, H. D. T. Mertens, P. V. Konarev, D. I. Svergun, New developments in the ATSAS program package for small-angle scattering data analysis. *J. Appl. Cryst.* **45**, 342–350 (2012).

94. D. Franke, M. V. Petoukhov, P. V. Konarev, A. Panjkovich, A. Tuukkanen, H. D. T. Mertens, A. G. Kikhney, N. R. Hajizadeh, J. M. Franklin, C. M. Jeffries, D. I. Svergun, *ATSAS 2.8*: A comprehensive data analysis suite for small-angle scattering from macromolecular solutions. *J. Appl. Cryst.* **50**, 1212–1225 (2017).

95. A. Panjkovich, D. I. Svergun, SASpy: A PyMOL plugin for manipulation and refinement of hybrid models against small angle x-ray scattering data. *Bioinformatics* **32**, 2062–2064 (2016).

96. E. F. Pettersen, T. D. Goddard, C. C. Huang, G. S. Couch, D. M. Greenblatt, E. C. Meng, T. E. Ferrin, UCSF Chimera—A visualization system for exploratory research and analysis. *J. Comput. Chem.* **25**, 1605–1612 (2004).

97. I. Horcas, R. Fernández, J. M. Gómez-Rodríguez, J. Colchero, J. Gómez-Herrero, A. M. Baro, WSXM: A software for scanning probe microscopy and a tool for nanotechnology. *Rev. Sci. Instrum.* **78**, 013705 (2007).

98. J. W. Slot, H. J. Geuze, Cryosectioning and immunolabeling. *Nat. Protoc.* **2**, 2480–2491 (2007).

99. H. Büeler, M. Fischer, Y. Lang, H. Bluethmann, H.-P. Lipp, S. J. De Armond, S. B. Prusiner, M. Aguet, C. Weissmann, Normal development and behaviour of mice lacking the neuronal cell-surface PrP protein. *Nature* **356**, 577–582 (1992).

100. M. Fischer, T. Rülicke, A. Raeber, A. Sailer, M. Moser, B. Oesch, S. Brandner, A. Aguzzi, C. Weissmann, Prion protein (PrP) with amino-proximal deletions restoring susceptibility of PrP knockout mice to scrapie. *EMBO J.* **15**, 1255–1264 (1996).

101. M. Marella, S. Lehmann, J. Grassi, J. Chabry, Filipin prevents pathological prion protein accumulation by reducing endocytosis and inducing cellular PrP release. *J. Biol. Chem.* **277**, 25457–25464 (2002).

102. J. I. Kim, K. Surewicz, P. Gambetti, W. K. Surewicz, The role of glycophosphatidylinositol anchor in the amplification of the scrapie isoform of prion protein in vitro. *FEBS Lett.* **583**, 3671–3675 (2009).

103. D. B. Freir, A. J. Nicoll, I. Klyubin, S. Panico, J. M. Mc Donald, E. Risse, E. A. Asante, M. A. Farrow, R. B. Sessions, H. R. Saibil, A. R. Clarke, M. J. Rowan, D. M. Walsh, J. Collinge, Interaction between prion protein and toxic amyloid β assemblies can be therapeutically targeted at multiple sites. *Nat. Commun.* **2**, 336 (2011).

104. M. V. Guillot-Sestier, C. Sunyach, S. T. Ferreira, M.-P. Marzolo, C. Bauer, A. Thevenet, F. Checler, α-Secretase-derived fragment of cellular prion, N1, protects against monomeric and oligomeric amyloid β (Aβ)-associated cell death. *J. Biol. Chem.* **287**, 5021–5032 (2012).

105. K. Nieznanski, J.-K. Choi, S. Chen, K. Surewicz, W. K. Surewicz, Soluble prion protein inhibits amyloid-β (Aβ) fibrillization and toxicity. *J. Biol. Chem.* **287**, 33104–33108 (2012).

106. B. R. Fluharty, E. Biasini, M. Stravalaci, A. Sclip, L. Diomede, C. Balducci, P. la Vitola, M. Messa, L. Colombo, G. Forloni, T. Borsello, M. Gobbi, D. A. Harris, An N-terminal fragment of the prion protein binds to amyloid-β oligomers and inhibits their neurotoxicity in vivo. *J. Biol. Chem.* **288**, 7857–7866 (2013).

107. J. Yuan, Y. A. Zhan, R. Abskharon, X. Xiao, M. C. Martinez, X. Zhou, G. Kneale, J. Mikol, S. Lehmann, W. K. Surewicz, J. Castilla, J. Steyaert, S. Zhang, Q. Kong, R. B. Petersen, A. Wohlkonig, W. Q. Zou, Recombinant human prion protein inhibits prion propagation in vitro. *Sci. Rep.* **3**, 2911 (2013).

108. J. J. Scott-McKean, K. Surewicz, J. K. Choi, V. A. Ruffin, A. I. Salameh, K. Nieznanski, A. C. S. Costa, W. K. Surewicz, Soluble prion protein and its N-terminal fragment prevent impairment of

synaptic plasticity by Aβ oligomers: Implications for novel therapeutic strategy in Alzheimer's disease. *Neurobiol. Dis.* **91**, 124–131 (2016).

109. E. Bove-Fenderson, R. Urano, J. E. Straub, D. A. Harris, Cellular prion protein targets amyloid-β fibril ends via its C-terminal domain to prevent elongation. *J. Biol. Chem.* **292**, 16858–16871 (2017).

110. E. Corda, X. du, S. Y. Shim, A. N. Klein, J. Siltberg-Liberles, S. Gilch, Interaction of peptide aptamers with prion protein central domain promotes α-cleavage of PrP^{C}. *Mol. Neurobiol.* **55**, 7758–7774 (2018).

111. F. L. Heppner, C. Musahl, I. Arrighi, M. A. Klein, T. Rülicke, B. Oesch, R. M. Zinkernagel, U. Kalinke, A. Aguzzi, Prevention of scrapie pathogenesis by transgenic expression of anti-prion protein antibodies. *Science* **294**, 178–182 (2001).

112. M. Enari, E. Flechsig, C. Weissmann, Scrapie prion protein accumulation by scrapie-infected neuroblastoma cells abrogated by exposure to a prion protein antibody. *Proc. Natl. Acad. Sci. U.S.A.* **98**, 9295–9299 (2001).

113. D. Peretz, R. A. Williamson, K. Kaneko, J. Vergara, E. Leclerc, G. Schmitt-Ulms, I. R. Mehlhorn, G. Legname, M. R. Wormald, P. M. Rudd, R. A. Dwek, D. R. Burton, S. B. Prusiner, Antibodies inhibit prion propagation and clear cell cultures of prion infectivity. *Nature* **412**, 739–743 (2001).

114. A. R. White, P. Enever, M. Tayebi, R. Mushens, J. Linehan, S. Brandner, D. Anstee, J. Collinge, S. Hawke, Monoclonal antibodies inhibit prion replication and delay the development of prion disease. *Nature* **422**, 80–83 (2003).

115. S. Gilch, F. Wopfner, I. Renner-Müller, E. Kremmer, C. Bauer, E. Wolf, G. Brem, M. H. Groschup, H. M. Schätzl, Polyclonal anti-PrP auto-antibodies induced with dimeric PrP interfere efficiently with PrPSc propagation in prion-infected cells. *J. Biol. Chem.* **278**, 18524–18531 (2003).

116. V. Perrier, J. Solassol, C. Crozet, Y. Frobert, C. Mourton-Gilles, J. Grassi, S. Lehmann, Anti-PrP antibodies block PrPSc replication in prion-infected cell cultures by accelerating PrPC degradation. *J. Neurochem.* **89**, 454–463 (2004).

117. G. Donofrio, F. L. Heppner, M. Polymenidou, C. Musahl, A. Aguzzi, Paracrine inhibition of prion propagation by anti-PrP single-chain Fv miniantibodies. *J. Virol.* **79**, 8330–8338 (2005).

118. J. Pankiewicz, F. Prelli, M. S. Sy, R. J. Kascsak, R. B. Kascsak, D. S. Spinner, R. I. Carp, H. C. Meeker, M. Sadowski, T. Wisniewski, Clearance and prevention of prion infection in cell culture by anti-PrP antibodies. *Eur. J. Neurosci.* **23**, 2635–2647 (2006).

119. C. H. Song, H. Furuoka, C. L. Kim, M. Ogino, A. Suzuki, R. Hasebe, M. Horiuchi, Effect of intraventricular infusion of anti-prion protein monoclonal antibodies on disease progression in prion-infected mice. *J. Gen. Virol.* **89**, 1533–1544 (2008).

120. M. J. Sadowski, J. Pankiewicz, F. Prelli, H. Scholtzova, D. S. Spinner, R. B. Kascsak, R. J. Kascsak, T. Wisniewski, Anti-PrP Mab 6D11 suppresses PrP(Sc) replication in prion infected myeloid precursor line FDC-P1/22L and in the lymphoreticular system in vivo. *Neurobiol. Dis.* **34**, 267–278 (2009).

121. A. Müller-Schiffmann, B. Petsch, S. Rutger Leliveld, J. Muyrers, A. Salwierz, C. Mangels, S. Schwarzinger, D. Riesner, L. Stitz, C. Korth, Complementarity determining regions of an anti-prion protein scFv fragment orchestrate conformation specificity and antiprion activity. *Mol. Immunol.* **46**, 532–540 (2009).

122. E. Chung, Y. Ji, Y. Sun, R. J. Kascsak, R. B. Kascsak, P. D. Mehta, S. M. Strittmatter, T. Wisniewski, Anti-PrPC monoclonal antibody infusion as a novel treatment for cognitive deficits in an Alzheimer's disease model mouse. *BMC Neurosci.* **11**, 130 (2010).

123. A. E. Barry, I. Klyubin, J. M. Mc Donald, A. J. Mably, M. A. Farrell, M. Scott, D. M. Walsh, M. J. Rowan, Alzheimer's disease brain-derived amyloid-β-mediated inhibition of LTP in vivo is prevented by immunotargeting cellular prion protein. *J. Neurosci.* **31**, 7259–7263 (2011).

124. N. Ohsawa, C. H. Song, A. Suzuki, H. Furuoka, R. Hasebe, M. Horiuchi, Therapeutic effect of peripheral administration of an anti-prion protein antibody on mice infected with prions. *Microbiol. Immunol.* **57**, 288–297 (2013).

125. I. Klyubin, A. J. Nicoll, A. Khalili-Shirazi, M. Farmer, S. Canning, A. Mably, J. Linehan, A. Brown, M. Wakeling, S. Brandner, D. M. Walsh, M. J. Rowan, J. Collinge, Peripheral administration of a humanized anti-PrP antibody blocks Alzheimer's disease Aβ synaptotoxicity. *J. Neurosci.* **34**, 6140–6145 (2014).

126. J. E. Pankiewicz, S. Sanchez, K. Kirshenbaum, R. B. Kascsak, R. J. Kascsak, M. J. Sadowski, Anti-prion protein antibody 6D11 restores cellular proteostasis of prion protein through disrupting recycling propagation of PrP^{Sc} and targeting PrP^{Sc} for lysosomal degradation. *Mol. Neurobiol.* **56**, 2073–2091 (2019).

127. T. O. Cox, E. C. Gunther, A. H. Brody, M. T. Chiasseu, A. Stoner, L. M. Smith, L. T. Haas, J. Hammersley, G. Rees, B. Dosanjh, M. Groves, M. Gardener, C. Dobson, T. Vaughan, I. Chessell, A. Billinton, S. M. Strittmatter, Anti-PrP^{C} antibody rescues cognition and synapses in transgenic Alzheimer mice. *Ann. Clin. Transl. Neurol.* **6**, 554–574 (2019).

128. C. Dyer, British man with CJD gets experimental treatment in world first. *BMJ* **363**, k4608 (2018).

129. I. Ferrer, R. Blanco, M. Carmona, B. Puig, R. Ribera, M. J. Rey, T. Ribalta, Prion protein expression in senile plaques in Alzheimer's disease. *Acta Neuropathol.* **101**, 49–56 (2001).

130. K. Schwarze-Eicker, K. Keyvani, N. Görtz, D. Westaway, N. Sachser, W. Paulus, Prion protein (PrPc) promotes β-amyloid plaque formation. *Neurobiol. Aging* **26**, 1177–1182 (2005).

131. C. Falker, A. Hartmann, I. Guett, F. Dohler, H. Altmeppen, C. Betzel, R. Schubert, D. Thurm, F. Wegwitz, P. Joshi, C. Verderio, S. Krasemann, M. Glatzel, Exosomal cellular prion protein drives fibrillization of amyloid beta and counteracts amyloid beta-mediated neurotoxicity. *J. Neurochem.* **137**, 88–100 (2016).

132. B. D. C. Boon, M. Bulk, A. J. Jonker, T. H. J. Morrema, E. van den Berg, M. Popovic, J. Walter, S. Kumar, S. J. van der Lee, H. Holstege, X. Zhu, W. E. van Nostrand, R. Natté, L. van der Weerd, F. H. Bouwman, W. D. J. van de Berg, A. J. M. Rozemuller, J. J. M. Hoozemans, The coarse-grained plaque: A divergent Aβ plaque-type in early-onset Alzheimer's disease. *Acta Neuropathol.* **140**, 811–830 (2020).

133. R. H. Takahashi, M. Yokotsuka, M. Tobiume, Y. Sato, H. Hasegawa, T. Nagao, G. K. Gouras, Accumulation of cellular prion protein within β-amyloid oligomer plaques in aged human brains. *Brain Pathol.* **31**, e12941 (2021).

134. L. J. Harris, S. B. Larson, K. W. Hasel, A. McPherson, Refined structure of an intact IgG2a monoclonal antibody. *Biochemistry* **36**, 1581–1597 (1997).